On Performance Limits of DFT Spread OFDM Systems

Muhammad Danish Nisar
Student Member IEEE,
Munich University of Technology (TUM)
80290 Munich, Germany
E-Mail: mdanishnisar@ieee.org

Hans Nottensteiner, Thomas Hindelang
Nokia Siemens Networks GmbH & Co. KG
Radio Access Research & Development
81617 Munich, Germany
{Hans.Nottensteiner, Thomas.Hindelang}@nsn.com

***Abstract*— DFT Spread OFDM has been proposed recently to reduce the Peak to Average Power Ratio (PAPR) of conventional OFDM transmission. Besides PAPR reduction, an important implication of DFT Spreading is that the independent parallel sub-channels between the sub-carriers cease to exist. This in turn leads to difference in its performance limits as compared to the conventional OFDM system. This paper analyzes the error probabilities of DFT Spread OFDM systems, and derives their analytical closed form expressions for the AWGN, fading AWGN, multipath and fading multipath channel scenarios. Simulation results presented in last section confirm the validity of the derived analytical expressions.**

I. Introduction

Orthogonal Frequency Division Multiplexing (OFDM) has proven to be an efficient underlying technology for wireless communication. The major motivation for OFDM comes from its relatively simple way of handling frequency selective channels which are normally encountered in wireless mobile systems [1], [2]. A major drawback of OFDM transmission, however, is its high *Peak to Average Power Ratio (PAPR)* which increases operational requirements of the Linear Power Amplifier in the transmitting equipment leading not only to an increased cost but also an increased power consumption which is not desired especially at the uplink transmitter, the *User Equipment (UE)*.

Numerous techniques have been developed to reduce OFDM PAPR [3], [4], [5] and *DFT Spread OFDM (DFT-SOFDM)* [6] is one outcome of such investigations. With an extra DFT block prior to the conventional OFDM transmitter, it proves to be an effective way of combining the benefits of OFDM with a low PAPR transmission signal. As such it has already been selected as the uplink modulation scheme for the upcoming Long Term Evolution of 3G systems under the work item of Evolved-UTRA by 3GPP [7].

Fig. 1 shows the principle of DFT SOFDM transmission applied to an uplink multiple access system whereby multiple users transform their time domain symbols independently via the DFT block to get the frequency domain sub-carriers. Each

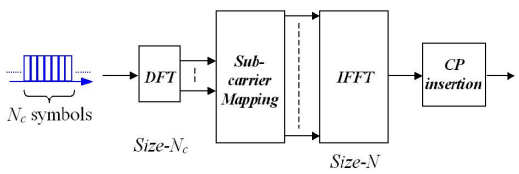

Fig. 1. DFT Spread OFDM Transmitter Structure

user then maps its sub-carriers onto a pre-assigned empty portion of the overall system spectrum followed by IFFT and CP insertion as in conventional OFDM transmission. Note that N_c represents the chunk size (the number of sub-carriers assigned to a user) and N is the total number of sub-carriers in the system.

Besides the PAPR reduction, an important implication of DFT Spreading is that the independent parallel sub-channels between the data symbols no longer exist. While in a conventional OFDM system each sub-channel can be considered as an AWGN channel with SNR determined by receiver noise and channel response at that sub-channel only, the idea cannot be applied to DFT-SOFDM. Analytical expressions for *Symbol Error Rate (SER)* and *Block or Packet Error Rate (PER)* can readily be found for OFDM optimal detection [8], but such an analysis can not be extended to the case of DFT-SOFDM optimum receiver.

In this paper, we analyze the error performance limits of DFT-SOFDM systems, starting with the case of ZF and MMSE equalizers. Analytical expressions for SER are derived for AWGN, fading AWGN, multipath and fading multipath channel scenarios. Finally we take a look at PER for the case of linear as well as the optimal (ML) detection and obtain closed form expression for an upper bound on PER.

II. System Model

We consider the transmission of a N_c dimensional symbol vector $\boldsymbol{s} \in \mathbb{C}^{N_c}$ which is transformed into the frequency domain leading to $\boldsymbol{X} = \boldsymbol{F}\boldsymbol{s} \in \mathbb{C}^{N_c}$, where $\boldsymbol{F} \in \mathbb{C}^{N_c \times N_c}$ is the unitary Fourier matrix i.e. $\boldsymbol{F}\boldsymbol{F}^{\mathrm{H}} = \boldsymbol{I}$. Now owing to the insertion of cyclic prefix of length ν greater than the length L of the channel impulse response, $\boldsymbol{h} \in \mathbb{C}^{L}$, and the IFFT and FFT operations of the transmitter and receiver respectively the following system model holds in the frequency domain [8],

$$\boldsymbol{Y} = \boldsymbol{H}\boldsymbol{X} + \boldsymbol{\eta} \tag{1}$$

where $\boldsymbol{H} \in \mathbb{C}^{N_c \times N_c}$ is a diagonal matrix containing the channel frequency response at the sub-carriers of interest i.e. $\boldsymbol{H} = \mathrm{diag}[\boldsymbol{F}_{N_c \times L}\boldsymbol{h}]$, $\boldsymbol{F}_{N_c \times L}$ is the respective portion of the Fourier matrix $\boldsymbol{F}_N \in \mathbb{C}^{N \times N}$. The vectors $\boldsymbol{Y}$ and $\boldsymbol{\eta} \in \mathbb{C}^{N_c}$ contain the received symbols and noise in the frequency domain. After the IDFT block at receiver, the system model above can be written in the data symbol domain as

$$\boldsymbol{y} = \boldsymbol{F}^{\mathrm{H}}\boldsymbol{H}\boldsymbol{F}\boldsymbol{s} + \boldsymbol{F}^{\mathrm{H}}\boldsymbol{\eta} \tag{2}$$

and with a linear equalizer $\boldsymbol{W} \in \mathbb{C}^{N_c \times N_c}$ in place, the reconstructed symbol can be expressed as

$$\hat{\boldsymbol{s}} = \boldsymbol{W}\boldsymbol{F}^{\mathrm{H}}\boldsymbol{H}\boldsymbol{F}\boldsymbol{s} + \boldsymbol{W}\acute{\boldsymbol{\eta}} \tag{3}$$

where $\acute{\boldsymbol{\eta}} = \boldsymbol{F}^{\mathrm{H}}\boldsymbol{\eta}$ is statistically equivalent to the original noise $\boldsymbol{\eta}$. Given the channel estimates, the equalizer can be designed under the ZF or MMSE criterion and can be given, for the case of uncorrelated noise $\boldsymbol{R}_{\eta} = \sigma_{\eta}^2\boldsymbol{I} = \boldsymbol{R}_{\acute{\eta}}$ and uncorrelated transmitted signal $\boldsymbol{R}_{\boldsymbol{s}} = \sigma_s^2\boldsymbol{I}$, as [9]

$$\boldsymbol{W}_{\mathrm{ZF}} = \boldsymbol{F}^{\mathrm{H}}\left(\boldsymbol{H}^{\mathrm{H}}\boldsymbol{H}\right)^{-1}\boldsymbol{H}^{\mathrm{H}}\boldsymbol{F} \tag{4}$$

$$\boldsymbol{W}_{\mathrm{MMSE}} = \boldsymbol{F}^{\mathrm{H}}\left(\frac{\sigma_{\eta}^2}{\sigma_s^2}\boldsymbol{I} + \boldsymbol{H}^{\mathrm{H}}\boldsymbol{H}\right)^{-1}\boldsymbol{H}^{\mathrm{H}}\boldsymbol{F} \tag{5}$$

III. SER Analysis

A. AWGN Channel

Since an AWGN channel correspond to a flat channel frequency response at all sub-carriers, the channel matrix under the channel energy constraint $\mathrm{E}\left[|H_i|^2\right] = 1$, reduces to an identity. The ZF equalizer, as such, is also an Identity matrix and its reconstruction expression can be given as

$$\hat{\boldsymbol{s}}_{\mathrm{ZF}} = \boldsymbol{s} + \acute{\boldsymbol{\eta}} \tag{6}$$

The MMSE equalizer for the under-consideration AWGN Channel reduces to a scaled identity i.e. $\boldsymbol{W}_{\mathrm{MMSE}} = \lambda\boldsymbol{I}$, with $\lambda = 1/(1+\sigma_{\eta}^2/\sigma_s^2)$ so that

$$\hat{\boldsymbol{s}}_{\mathrm{MMSE}} = \lambda\left(\boldsymbol{s} + \acute{\boldsymbol{\eta}}\right) \tag{7}$$

We note that for the case of uncorrelated noise, both ZF and MMSE reconstructions simplify to scalar equations and both have the same symbol error probability (SER), that can be given as [8],

$$\mathrm{P}_{\mathrm{MMSE}} = \mathrm{P}_{\mathrm{ZF}} = \Pr(s_i \neq \hat{s}_i) = Q\left(\sqrt{\frac{2E_s}{N_o}}\right) \tag{8}$$

B. Fading AWGN Channel

The channel frequency response is still flat but the amplitude no longer remains fixed at 1, rather it varies (say in accordance with rayleigh fading) from one channel realization to other. The diagonal channel matrix is assumed to be $\boldsymbol{H} = \rho\boldsymbol{I}$ with $\mathrm{E}\left[|\rho|^2\right] = 1$, to satisfy the energy constraint. The ZF equalizer in this case reads as $\boldsymbol{W}_{\mathrm{ZF}} = (1/\rho)\boldsymbol{I}$ so that,

$$\hat{\boldsymbol{s}}_{\mathrm{ZF}} = \boldsymbol{s} + (1/\rho)\acute{\boldsymbol{\eta}} \tag{9}$$

and as such its SER can be given as

$$\mathrm{P}_{\mathrm{ZF}} = \Pr(s_i \neq \hat{s}_i) = \mathrm{E}_H\left[Q\left(\sqrt{\frac{2E_s|\rho|^2}{N_o}}\right)\right] \tag{10}$$

The MMSE equalizer again simplifies to a scaled identity i.e. $\boldsymbol{W}_{\mathrm{MMSE}} = \lambda\boldsymbol{I}$, with $\lambda = \rho^*/(|\rho|^2 + \sigma_{\eta}^2/\sigma_s^2)$ so that,

$$\hat{\boldsymbol{s}}_{\mathrm{MMSE}} = \lambda\rho\boldsymbol{s} + \lambda\acute{\boldsymbol{\eta}} \tag{11}$$

leading to the same SER expression as for ZF, i.e. $\mathrm{P}_{\mathrm{MMSE}} = \mathrm{P}_{\mathrm{ZF}}$ from (10).

C. Multipath Channel

Now we come to the more interesting case of multipath channels, where the channel matrix is an arbitrary diagonal matrix but still with the energy constraint $\mathrm{E}\left[|H_i|^2\right] = 1$. The ZF reconstruction expression can be written as

$$\hat{\boldsymbol{s}} = \boldsymbol{s} + \boldsymbol{F}^{\mathrm{H}}\left(\boldsymbol{H}^{\mathrm{H}}\boldsymbol{H}\right)^{-1}\boldsymbol{H}^{\mathrm{H}}\boldsymbol{\eta} = \boldsymbol{s} + \grave{\boldsymbol{\eta}} \tag{12}$$

where $\grave{\eta}_i$, the i_{th} effective noise component given as,

$$\grave{\eta}_i = \sum_{j=1}^{N_o}\left(\frac{F_{j,i}^*}{H_j}\right)\eta_j \tag{13}$$

has a mean of zero, and its variance can be given as,

$$\sigma_{\grave{\eta}_i}^2 = \sigma_{\eta}^2\sum_{j=1}^{N_o}\left|\frac{F_{j,i}^*}{H_j}\right|^2 = \sigma_{\eta}^2\left(\frac{1}{N_c}\sum_{j=1}^{N_o}\frac{1}{|H_j|^2}\right) = \beta_{\mathrm{ZF}}\ \sigma_{\eta}^2 \tag{14}$$

where β_{ZF} can be termed as the ZF noise amplification factor. It is worth appreciating here that $\sigma_{\grave{\eta}_i}^2 = \sigma_{\grave{\eta}}^2$ is independent of the index i, and as such unlike the case of conventional OFDM, all the symbols are equally likely to be in error. Because of the presence of DFT spreading, the different sub-channel SNRs in the frequency domain are averaged to a constant SNR in the data-symbol domain. The SER for a symbol-wise slicer can be expressed as

$$\mathrm{P}_{\mathrm{ZF}} = \Pr(s_i \neq \hat{s}_i) = Q\left(\sqrt{\frac{2E_s}{\beta_{\mathrm{ZF}}N_0}}\right) \tag{15}$$

The MMSE equalizer's reconstruction reads as

$$\hat{\boldsymbol{s}} = \boldsymbol{F}^{\mathrm{H}}\left(\frac{\sigma_{\eta}^2}{\sigma_s^2}\boldsymbol{I} + \boldsymbol{H}^{\mathrm{H}}\boldsymbol{H}\right)^{-1}\boldsymbol{H}^{\mathrm{H}}\boldsymbol{H}\boldsymbol{F}\boldsymbol{s} + \boldsymbol{F}^{\mathrm{H}}\left(\frac{\sigma_{\eta}^2}{\sigma_s^2}\boldsymbol{I} + \boldsymbol{H}^{\mathrm{H}}\boldsymbol{H}\right)^{-1}\boldsymbol{H}^{\mathrm{H}}\boldsymbol{\eta} \tag{16}$$

and we proceed now by analyzing the noise, the desired signal and the interference power at the equalizer output. The i_{th} effective noise component can now be given as,

$$\grave{\eta}_i = \sum_{j=1}^{N_o}\left(\frac{F_{j,i}^*H_j^*}{|H_j|^2 + \sigma_{\eta}^2/\sigma_s^2}\right)\eta_j \tag{17}$$

and can be shown to have a mean of zero, and variance

$$\sigma_{\grave{\eta}_i}^2 = \sigma_{\eta}^2\left(\frac{1}{N_c}\sum_{j=1}^{N_o}\left(\frac{|H_j|}{|H_j|^2 + \sigma_{\eta}^2/\sigma_s^2}\right)^2\right) = \beta_{\mathrm{MMSE}}\ \sigma_{\eta}^2 \tag{18}$$

where β_{MMSE} can be termed as the noise amplification factor for the MMSE equalizer and can be shown to be less than β_{ZF}. Note again that $\sigma_{\grave{\eta}_i}^2 = \sigma_{\grave{\eta}}^2$ is independent of the index i, and as such all symbols experience the same noise power. Nevertheless the noise covariance matrix can be shown to have a non-diagonal structure indicating some degree of correlation between the various noise components.

Examining the reconstruction expression in (16) further, we note that the signal vector is being operated on by the matrix $\boldsymbol{A} = \boldsymbol{W}_{\mathrm{MMSE}}\boldsymbol{F}^{\mathrm{H}}\boldsymbol{H}\boldsymbol{F}$, whose entry in i_{th} row and k_{th} column can be shown to be

$$a_{i,k} = \sum_{j=1}^{N_o}\frac{F_{j,i}^*F_{j,k}\,|H_j|^2}{|H_j|^2 + \sigma_{\eta}^2/\sigma_s^2} \tag{19}$$

The diagonal entries of this matrix which scale the desired symbol, simplify to

$$a_{i,i} = \frac{1}{N_c}\sum_{j=1}^{N_c}\frac{|H_j|^2}{|H_j|^2 + \sigma_\eta^2/\sigma_s^2} \tag{20}$$

The effective desired signal power at the equalizer output can therefore be given as

$$\sigma_D^2 = \sigma_s^2\left(\frac{1}{N_c}\sum_{j=1}^{N_c}\frac{|H_j|^2}{|H_j|^2 + \sigma_\eta^2/\sigma_s^2}\right)^2 = \alpha_{\text{MMSE}}\ \sigma_s^2 \tag{21}$$

where α_{MMSE} can be described as the desired signal amplification factor. Note that the MMSE equalizer also accumulates some interference power that can be given for the i_{th} symbol as

$$\begin{aligned}\sigma_{I_i}^2 &= \sigma_s^2\left(\sum_{k=1}^{N_c}|a_{i,k}|^2 - |a_{i,i}|^2\right)\\ &= \sigma_s^2\left(\frac{1}{N_c}\sum_{j=1}^{N_c}\left(\frac{|H_j|^2}{|H_j|^2 + \sigma_\eta^2/\sigma_s^2}\right)^2 - \alpha_{\text{MMSE}}\right)\\ &= \gamma_{\text{MMSE}}\ \sigma_s^2\end{aligned} \tag{22}$$

Interestingly, we note that the interference amplification factor γ_{MMSE} in (22), the desired signal amplification factor α_{MMSE} in (21) and the noise amplification factor β_{MMSE} in (18) are all independent of the symbol index i. All the symbols are therefore expected to have the same error probability. Finally we note that the noise and interference powers from (18) and (22) can be combined to get,

$$\begin{aligned}\sigma_{\eta_i}^2 + \sigma_{I_i}^2 &= \frac{\sigma_s^2}{N_c}\left(\sum_{j=1}^{N_c}\left(\frac{|H_j|\,\sigma_\eta/\sigma_s}{|H_j|^2 + \sigma_\eta^2/\sigma_s^2}\right)^2 + \sum_{j=1}^{N_c}\left(\frac{|H_j|^2}{|H_j|^2 + \sigma_\eta^2/\sigma_s^2}\right)^2\right)\\ &\quad - \alpha_{\text{MMSE}}\ \sigma_s^2\\ &= \frac{\sigma_s^2}{N_c}\left(\sum_{j=1}^{N_c}\left(\frac{|H_j|^2\left(\sigma_\eta^2/\sigma_s^2 + |H_j|^2\right)}{\left(|H_j|^2 + \sigma_\eta^2/\sigma_s^2\right)^2}\right)\right) - \alpha_{\text{MMSE}}\ \sigma_s^2\\ &= \sigma_s^2\left(\sqrt{\alpha_{\text{MMSE}}} - \alpha_{\text{MMSE}}\right)\end{aligned} \tag{23}$$

so that the SER expression for the MMSE equalizer, under the loose assumption of interference being gaussian, can be given as

$$\begin{aligned}\text{P}_{\text{MMSE}} = \Pr(s_i \neq \hat{s}_i) &= Q\left(\sqrt{\frac{\sigma_D^2}{\sigma_\eta^2 + \sigma_I^2}}\right)\\ &= Q\left(\sqrt{\frac{1}{\sqrt{1/\alpha_{\text{MMSE}}} - 1}}\right)\end{aligned} \tag{24}$$

D. Multipath Fading Channel

The analysis in the last sub-section for multipath channels can easily be extended for the time varying (fading) multipath channels. We note from the ZF and MMSE SER equations (15) and (24), that β_{ZF} and α_{MMSE} are dependent on the channel realization. So we obtain the SER expressions for the fading multipath channels by introducing an expectation operator in respective equations for non-fading channels. Thus we have

$$\text{P}_{\text{ZF}} = \text{E}_H\left[Q\left(\sqrt{\frac{2E_s}{\beta_{\text{ZF}}N_0}}\right)\right] \tag{25}$$

$$\text{P}_{\text{MMSE}} = \text{E}_H\left[Q\left(\sqrt{\frac{1}{\sqrt{1/\alpha_{\text{MMSE}}} - 1}}\right)\right] \tag{26}$$

IV. PER Analysis

For the Block or Packet error rate, we introduce two solutions. First, we note that for detection via ZF or MMSE equalizer we may use the union bound [10] to arrive at an upper bound on PER as follows,

$$\begin{aligned}\Pr(\boldsymbol{s} \neq \hat{\boldsymbol{s}}) &= \Pr(\hat{s}_1 \neq s_1 \cup \hat{s}_2 \neq s_2 \cup \ldots \cup \hat{s}_{N_c} \neq s_{N_c})\\ &\leq \sum_{i=1}^{N_c}\Pr(s_i \neq \hat{s}_i)\end{aligned} \tag{27}$$

Plugging in the appropriate SER expression in above equation gives a reasonably tight upper bound on the PER especially at high SNRs.

We now turn our attention to the PER of optimal ML detector operating directly on the received data symbols $\boldsymbol{y}$

$$\boldsymbol{y} = \boldsymbol{F}^{\text{H}}\boldsymbol{H}\boldsymbol{F}\boldsymbol{s} + \boldsymbol{F}^{\text{H}}\boldsymbol{\eta} = \acute{\boldsymbol{H}}\boldsymbol{s} + \acute{\boldsymbol{\eta}} \tag{28}$$

The full-blown ML detector chooses $\hat{\boldsymbol{s}}$ that maximizes the likelihood, i.e.

$$\hat{\boldsymbol{s}} = \underset{\boldsymbol{s}_i}{\text{argmax}}\{\text{P}\ (\boldsymbol{y}|\acute{\boldsymbol{H}}, \boldsymbol{s}_i) = \text{P}_\eta(\boldsymbol{y} - \acute{\boldsymbol{H}}\boldsymbol{s}_i)\} = \underset{\boldsymbol{s}_i}{\text{argmin}}\ \Gamma_i(\boldsymbol{y}) \tag{29}$$

so it needs to compute the following metrics

$$\Gamma_i(\boldsymbol{y}) = \left\|\boldsymbol{y} - \acute{\boldsymbol{H}}\boldsymbol{s}_i\right\|_2^2 \text{ for } i = 1, 2, \ldots, M = C^{N_c} \tag{30}$$

and chooses $\hat{\boldsymbol{s}} = \boldsymbol{s}_i$ that leads to the minimum metric. Note that C is the constellation size. The ML detector makes an error if say $\boldsymbol{s}_1$ was transmitted and $\Gamma_1(\boldsymbol{y})$ is not the minimum. Thus the PER in case of equiprobable transmissions can be written as

$$\begin{aligned}\Pr(\boldsymbol{s} \neq \hat{\boldsymbol{s}}) &= \Pr(\Gamma_1 \not< \Gamma_2, \Gamma_3, \ldots, \Gamma_M|\mathcal{H}_1)\\ &= 1 - \Pr(\Gamma_1 < \Gamma_2 \cap \Gamma_1 < \Gamma_3 \cap \ldots \cap \Gamma_1 < \Gamma_M|\mathcal{H}_1)\end{aligned} \tag{31}$$

where $\mathcal{H}_1$ represents the hypothesis that $\boldsymbol{s}_1$ was transmitted. Next we determine the $\Pr(\Gamma_1 < \Gamma_j|\mathcal{H}_1)$, by first defining a new variable

$$\begin{aligned}\tau &= (\Gamma_1 - \Gamma_j)|\mathcal{H}_1\\ &= -[\boldsymbol{\Delta s}^{\text{H}}\acute{\boldsymbol{H}}^{\text{H}}\acute{\boldsymbol{H}}\boldsymbol{\Delta s} + \boldsymbol{\Delta s}^{\text{H}}\acute{\boldsymbol{H}}^{\text{H}}\acute{\boldsymbol{\eta}} + \acute{\boldsymbol{\eta}}^{\text{H}}\acute{\boldsymbol{H}}\boldsymbol{\Delta s}]\end{aligned} \tag{32}$$

where $\boldsymbol{\Delta s} = \boldsymbol{s}_1 - \boldsymbol{s}_j$. The moments of this new gaussian variable τ are computed to be,

$$\mu_\tau = -\boldsymbol{\Delta s}^{\text{H}}\acute{\boldsymbol{H}}^{\text{H}}\acute{\boldsymbol{H}}\boldsymbol{\Delta s} \tag{33}$$

$$\sigma_\tau^2 = 2\sigma_{\acute{\eta}}^2\boldsymbol{\Delta s}^{\text{H}}\acute{\boldsymbol{H}}^{\text{H}}\acute{\boldsymbol{H}}\boldsymbol{\Delta s} = -2\sigma_{\acute{\eta}}^2\mu_\tau \tag{34}$$

Thus we have $\tau \sim \mathcal{N}(\mu_\tau, \sigma_\tau^2)$ and as such

$$\Pr(\Gamma_1 < \Gamma_j|\mathcal{H}_1) = \Pr(\tau < 0) = 1 - Q\left(\sqrt{\frac{\boldsymbol{\Delta s}^{\text{H}}\acute{\boldsymbol{H}}^{\text{H}}\acute{\boldsymbol{H}}\boldsymbol{\Delta s}}{2\sigma_{\acute{\eta}}^2}}\right) \tag{35}$$

we note however that (31) can be expanded in terms of these individual probabilities only if the metrics Γ_i are independent, which is not the case here. In our case we can only expand it in terms of following conditional probabilities,

$$\begin{aligned}\Pr(s \neq \hat{s}) &= 1 - \Pr(\Gamma_1 < \Gamma_2 \cap \Gamma_1 < \Gamma_3 \cap \ldots \cap \Gamma_1 < \Gamma_M|\mathcal{H}_1)\\ &= 1 - \Pr(\Gamma_1 < \Gamma_2|\mathcal{H}_1)\Pr(\Gamma_1 < \Gamma_3|\Gamma_1 < \Gamma_2, \mathcal{H}_1)\ldots\\ &\quad \ldots\Pr(\Gamma_1 < \Gamma_M|\Gamma_1 < \Gamma_2, \Gamma_1 < \Gamma_3, \ldots, \Gamma_1 < \Gamma_{M-1}, \mathcal{H}_1)\end{aligned} \tag{36}$$

Next we argue that the first term in the product would be much higher than other probabilities which condition already that

$\Gamma_1 < \Gamma_k$ for some k's. This upper bound on PER can be even strengthened by considering one of the nearest neighbours of $\boldsymbol{s}_1$ in the first place, so that we have

$$\Pr(\boldsymbol{s} \neq \hat{\boldsymbol{s}}) \leq 1 - [\Pr(\Gamma_1 < \Gamma_{\text{nearest}} | \mathcal{H}_1)]^{M-1} \tag{37}$$

where the $\Pr(\Gamma_1 < \Gamma_{\text{nearest}} | \mathcal{H}_1)$ can be evaluated using (35) with $\boldsymbol{\Delta s} = \sqrt{2E_s}\boldsymbol{e}_p$, where $\boldsymbol{e}_p$ is a vector with a one at p_{th} place and zeros elsewhere, so that

$$\begin{aligned} \boldsymbol{\Delta s}^{\mathrm{H}} \acute{\boldsymbol{H}}^{\mathrm{H}} \acute{\boldsymbol{H}} \boldsymbol{\Delta s} &= 2E_s \boldsymbol{e}_p{}^{\mathrm{H}} \left(\boldsymbol{F}^{\mathrm{H}} \boldsymbol{H} \boldsymbol{F} \right)^{\mathrm{H}} \left(\boldsymbol{F}^{\mathrm{H}} \boldsymbol{H} \boldsymbol{F} \right) \boldsymbol{e}_p \\ &= 2E_s \boldsymbol{e}_p{}^{\mathrm{H}} \boldsymbol{F}^{\mathrm{H}} \boldsymbol{H}^{\mathrm{H}} \boldsymbol{H} \boldsymbol{F} \boldsymbol{e}_p \\ &= \frac{2E_s}{N_c} \sum_{i=1}^{N_c} |H_i|^2 \end{aligned} \tag{38}$$

Hence, we finally have the upper bound on PER, that can be expressed as follows,

$$\Pr(\boldsymbol{s} \neq \hat{\boldsymbol{s}}) \leq 1 - \left[1 - Q\left(\sqrt{\frac{2E_s}{N_o} \frac{1}{N_c} \sum_{i=1}^{N_c} |H_i|^2} \right) \right]^{M-1} \tag{39}$$

V. Simulation Results

A comparison of the derived analytical formulas for the SER for different channel scenarios is made to the simulation results. The system under consideration operates over a 20 MHz bandwidth with 2048 subcarriers, and the number of sub-carriers assigned to the user under-consideration is N_c=25. These simulation parameters are adopted from E-UTRA specs [7]. Vehicular A channel profile [11] is used for comparing simulation and analytical results for a multipath channel. Rayleigh fading has been adopted to analyze the performance for fading scenarios.

The SER expressions derived for the case of AWGN channel are found to be in complete agreement to the simulation results in Figure 2. Moreover it needs to be emphasized that the performance of DFT-SOFDM over AWGN channel is identical to that of conventional OFDM systems [8]. Figure 3 shows the performance over multipath channel, where again the agreement of the derived analytical expressions and simulated results is exceptionally close.

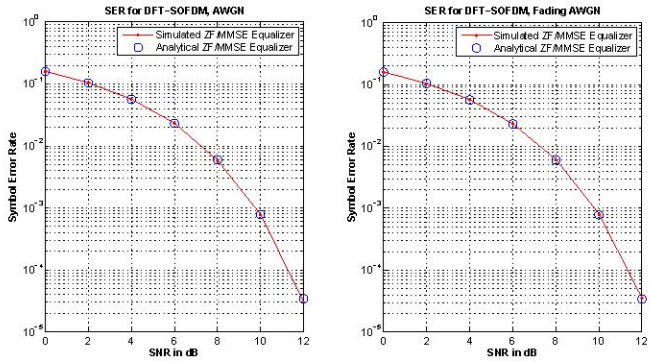

Fig. 2. AWGN Channel with and without fading

Figure 4 depicts the performance results in terms of the Packet Error Rate (PER). The union bound can be seen to be quite a tight upper bound on PER especially at low PERs. At high PERs, the approximation based ML upper bound proves to be tighter than the union bound.

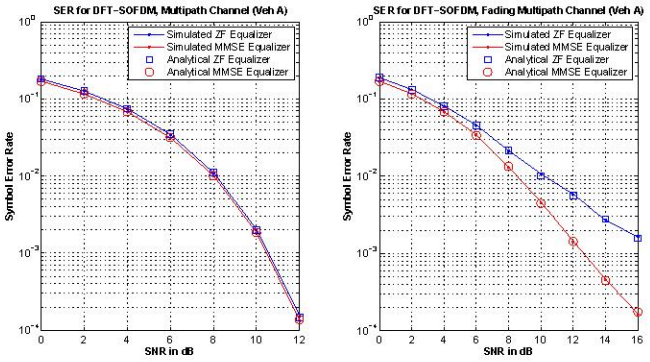

Fig. 3. Multipath Channel with and without fading

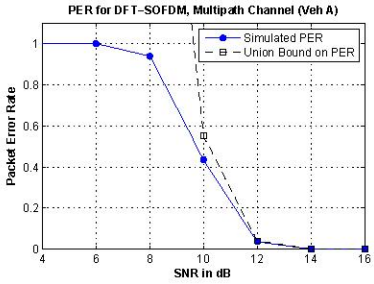

Fig. 4. PER on a Multipath Channel

VI. Conclusion

In this paper, we analyzed the error performance limits of DFT Spread OFDM systems. Besides the reasonably close bounds on packet error rate for the case of optimal ML detection, we derived closed form analytical expressions of the symbol error rate for the case of ZF and MMSE equalization under both AWGN and multipath channels. The complete agreement of the simulation results, presented in the last section, with the analytical ones confirm the validity of the derived expressions.

References

[1] J. A. Bingham, "Multicarrier modulation for data transmission: An idea whose time has come," *IEEE Communication Magazine*, May 1990.

[2] J. M. Cioffi, "A multicarrier primer," *Online, http://www.stanford.edu/group/cioffi/pdf/multicarrier.pdf*, 1991.

[3] P. V. Eetvelt, G. Wade, and M. Tomlinson, "Peak to average power reduction for OFDM schemes by selective scrambling," in *Electronic Letters*, Oct 1996, vol. 32, pp. 1963–1964.

[4] D. Wulich and L. Goldfeld, "Reduction of peak factor in orthogonal multicarrier modulation by amplitude limiting and coding," in *IEEE Trans. Commun.*, 1999, vol. 47, pp. 18–21.

[5] M. Breiling, S. H. Mller, and J. B. Huber, "Peak power reduction in OFDM without explicit side information," in *Proc. of International OFDM workshop 2000, Hamburg*, Sep 2000.

[6] D. Galda and H. Rohling, "A low complexity transmitter structure for OFDM-FDMA uplink systems," in *Vehicular Technology Conference*, 2002, pp. 1737–1741.

[7] Standardization Committee 3GPP, "Physical layer aspects for E-UTRA, 3GPP TR 25.814," *Online, http://3gpp.org*, 2006.

[8] L. Hanzo, M. Mnster, B. J. Choi, and T. Keller, *OFDM and MC-CDMA for Broadband Multiuser communications, WLANS and Broadcasting*, IEEE press and Wiley, 2003.

[9] M. Danish Nisar, *Channel Estimation and Equalization for Evolved UTRA Uplink*, Master thesis, Munich University of Technology, TUM, Germany, Oct 2006.

[10] Thomas. M. Cover and Joy. A. Thomas, *Elements of Information Theory*, John Wiley, 1991.

[11] Standardization Committee ITU, "Guidelines for evaluation of radio transmission technologies for IMT-2000," *ITU-R Rec. M. 1225*.